Lawrence Berkeley National Laboratory
Lawrence Berkeley National Laboratory

Title

Self- and dopant diffusion in extrinsic boron doped isotopically controlled silicon multilayer structures

Permalink

https://escholarship.org/uc/item/8xz2s339

Authors

Sharp, Ian D.
Bracht, Hartmut A.
Silvestri, Hughes H.
et al.

Publication Date

2002-04-01

eScholarship.org Powered by the California Digital Library
University of California

Self- and Dopant Diffusion in Extrinsic Boron Doped Isotopically Controlled Silicon Multilayer Structures

Ian D. Sharp,[a,b] Hartmut A. Bracht,[c] Hughes H. Silvestri,[a,b] Samuel P. Nicols,[a,b] Jeffrey W. Beeman,[b] John L. Hansen,[d] Arne Nylandsted Larsen,[d] and Eugene E. Haller[a,b]
[a]Department of Materials Science, University of California, Berkeley, CA 94720
[b]Materials Sciences Division, Lawrence Berkeley National Laboratory, Berkeley, CA 94720
[c]Institut für Materialphysik, Universität Münster, D 48149 Münster, Germany
[d]Institute of Physics and Astronomy, University of Aarhus, DK 8000 Aarhus, Denmark

ABSTRACT

Isotopically controlled silicon multilayer structures were used to measure the enhancement of self- and dopant diffusion in extrinsic boron doped silicon. ^{30}Si was used as a tracer through a multilayer structure of alternating natural Si and enriched ^{28}Si layers. Low energy, high resolution secondary ion mass spectrometry (SIMS) allowed for simultaneous measurement of self- and dopant diffusion profiles of samples annealed at temperatures between 850°C and 1100°C. A specially designed ion-implanted amorphous Si surface layer was used as a dopant source to suppress excess defects in the multilayer structure, thereby eliminating transient enhanced diffusion (TED) behavior. Self- and dopant diffusion coefficients, diffusion mechanisms, and native defect charge states were determined from computer-aided modeling, based on differential equations describing the diffusion processes. We present a quantitative description of B diffusion enhanced self-diffusion in silicon and conclude that the diffusion of both B and Si is mainly mediated by neutral and singly positively charged self-interstitials under p-type doping. No significant contribution of vacancies to either B or Si diffusion is observed.

INTRODUCTION

The aim of this study is to reveal the mechanism of self- and dopant diffusion in boron doped extrinsic Si. Knowledge of the diffusion mechanism will allow for the development of a comprehensive and predictive diffusion model that is based upon physically justifiable parameters. This fundamental understanding of self- and dopant diffusion may help reduce diffusion-related problems associated with increasingly shallow and highly doped junctions. Simultaneous analysis of self- and dopant diffusion will also reveal information about the process of self-diffusion in intrinsic Si.

Historically, Si self-diffusion experiments have been carried out using the radioactive isotope tracer ^{31}Si [1-4]. Due to the short half-life of ^{31}Si ($t_{1/2}$ = 2.6 h), the usefulness of these experiments was limited to short diffusion anneals at high temperatures. In recent years, highly enriched and chemically pure stable isotopes have become available. Stable isotope tracers allow for annealing times of any length over much broader temperature ranges, thereby increasing the accuracy of experimental results. These stable isotopes have been successfully used for intrinsic Si self-diffusion experiments [5,6] and preliminary studies on self-diffusion in extrinsic Si [7,8].

Simultaneous measurement of B and Si diffusion profiles using secondary ion mass spectrometry (SIMS), in conjunction with computer modeling techniques, is used to determine the charge states and relative contributions of native defects to Si and B diffusion. The

concentrations of neutral defects are independent of the Fermi level but charged defect concentrations strongly depend on the Fermi level position [9]. Therefore, simultaneous analysis of self- and dopant diffusion is essential to the formulation of a quantitative defect-assisted diffusion model.

Effects arising from ion implantation (e.g., TED), oxidation (interstitial wind), and nitridation (vacancy wind), must be alleviated for this experiment to accurately isolate and reveal the Fermi level effect. These three effects have been extensively studied [10,11] and are not the subject of the current research. Additional experiments and calculations were performed to confirm that these effects are, indeed, negligible in our multilayer structures.

EXPERIMENTAL DETAILS

Alternating layers of natural Si (92.2% ^{28}Si, 4.7% ^{29}Si, 3.1% ^{30}Si) and isotopically enriched ^{28}Si (99.95% ^{28}Si) were grown via ultra high vacuum chemical vapor deposition (UHV-CVD) at Lawrence Semiconductor Research Laboratory (Tempe, AZ) on a (100) natural Si substrate. A total of ten 120 nm thick layers were grown to form the isotopically controlled diffusion structure. A 200 nm thick natural Si cap layer was grown on top of the multilayer structure. To form a dopant source, a 250 nm thick amorphous natural Si layer was grown via molecular beam epitaxy (MBE) at the University of Aarhus (Denmark) on top of the crystalline isotope multilayer structure and ion-implanted with boron at a dose of $7\text{x}10^{15}$ cm^{-2} at 32 keV and $1\text{x}10^{16}$ cm^{-2} at 37 keV. Figure 1(a) shows the implanted multilayer structure prior to annealing. The implanted sample was diced into 4x4 mm^2 samples for annealing and cleaned in heated xylenes and acetone and room temperature methanol. Surface oxide was removed from the sample surfaces via a 30 s etch in concentrated HF. Silica ampoules were etched for 5 min in 5% HF. The samples were placed in the ampoules and evacuated to a base pressure of $1\text{-}2\text{x}10^{-5}$ Torr. Prior to sealing, the ampoules were backfilled with Ar to approximately 180 Torr. Samples were annealed for various times at temperatures between 845 ^{o}C and 1098 ^{o}C in a $\pm$2 K temperature controlled tube furnace.

Concentration versus depth data were simultaneously collected for ^{30}Si, ^{28}Si, and ^{11}B using a 1 keV oxygen beam on an ATOMIKA 4500 SIMS instrument at Accurel Systems (Sunnyvale, CA). The differential equations governing diffusion in this system were solved using a specially adapted version of the partial differential equation solver ZOMBIE [12].

To verify that TED was not present in these experiments, additional samples were implanted with Si at a dose of $7\text{x}10^{15}$ cm^{-2} at 50 keV and $1\text{x}10^{16}$ cm^{-2} at 65 keV. These samples were then prepared, annealed, and analyzed as described above. The results of ZOMBIE modeling were compared to intrinsic results to determine if TED effects were present.

RESULTS

Two interstitial mediated diffusion mechanisms, the kick-out mechanism [13] (Eq. 1) and the interstitialcy mechanism [14,15] (Eq. 2) have been proposed for B diffusion in Si:

$$\mathbf{B_i} \leftrightarrow \mathbf{B_s} + \boldsymbol{I} \tag{1}$$

$$[\mathbf{B}\boldsymbol{I}] \leftrightarrow \mathbf{B_s} + \boldsymbol{I} \tag{2}$$

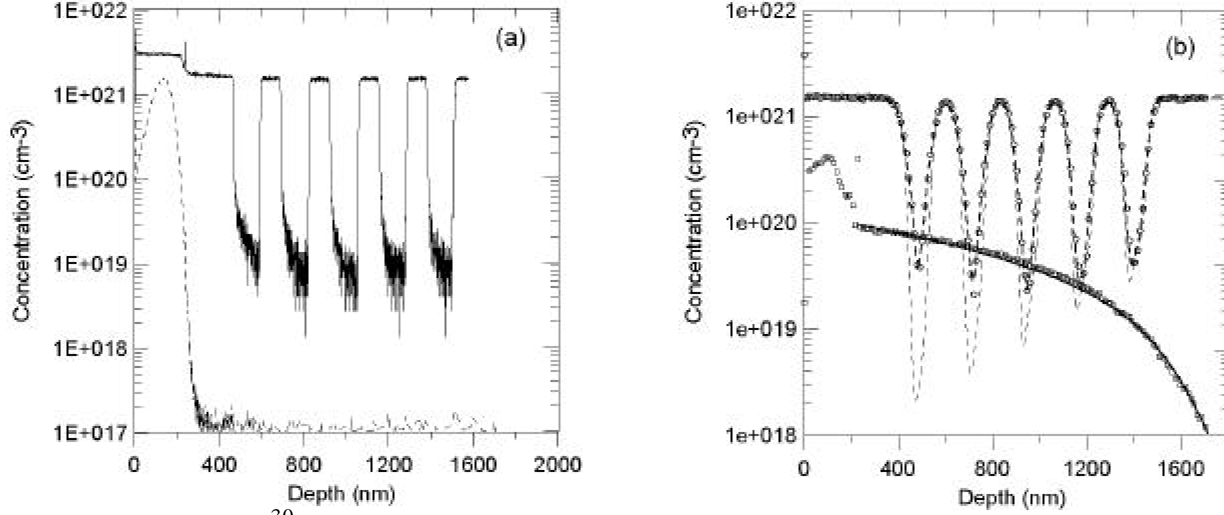

Figure 1: (a) SIMS ^{30}Si (solid line) and B (dashed line) profiles of a B implanted Si isotope multilayer structure prior to annealing. (b) SIMS ^{30}Si (❍) and B (ð) profiles after annealing for 4hr 55min at 1000 ^{o}C. Only every twentieth data point is shown for clarity. Simulation results for ^{30}Si (bold dashed line) and B (bold solid line) are in close agreement with experimental data. Comparison of the data to the simulated intrinsic diffusion profile (dashed line) reveals greater diffusion enhancement at higher B concentrations.

where the subscripts *s* and *i* refer to substitutional and interstitial boron, respectively, and *I* refers to self-interstitial atoms. Additional equations for both of these general mechanisms exist which take into account defect charge states mediating self- and dopant diffusion.

A variety of simulations were conducted for various combinations of defect charge states and reaction mechanisms. Figure 1(b) shows the ^{30}Si and B SIMS concentration profiles along with ZOMBIE simulated diffusion profiles for the two species. Simulation results, such as those shown in Figure 1(b), revealed self- and dopant diffusion to be mediated by neutral and singly positively charged self-interstitials, via the mechanisms given by Eqs. 3 and 4:

$$\mathbf{B_i^0 \Leftrightarrow B_s^- + \mathit{I}^0 + h} \quad (3)$$

$$\mathbf{B_i^0 \Leftrightarrow B_s^- + \mathit{I}^+} \,. \quad (4)$$

No significant contribution to Si and B diffusion from vacancies (V) was observed. This is a consequence of the B diffusion process, which creates a supersaturation of self-interstitials resulting in an undersaturation of vacancies. Accordingly, the contribution of vacancies to Si and B diffusion is suppressed. In the case that the interstitialcy mechanism mediates B diffusion, the diffusion of the $[BI]^0$ pair also contributes to Si self-diffusion. However, simulation of the B and Si diffusion profiles does not reveal a significant contribution of $[BI]^0$ to Si self-diffusion. Hence, either the kick-out mechanism controls B diffusion or the correlation factor for Si diffusion via $[BI]^0$ pairs is equal to or less than 0.3. Since such a low correlation factor is rather unlikely, B diffusion is considered to be mediated by the kick-out mechanism.

Self- and dopant diffusivity enhancements increased with increasing B doping due to I^0 and I^+ supersaturation from B diffusion and I^+ concentration enhancement due to the Fermi level effect. As expected, the contribution of I^0 is independent of the Fermi level and the contribution of I^+ increases as the Fermi level moves towards the valence band edge.

No self-diffusion enhancement was observed in Si implanted multilayer structures after annealing. Diffusivities extracted from simulation of the corresponding SIMS profiles are in excellent agreement with intrinsic diffusivities given in the literature [5]. Therefore, the experimentally observed enhanced self-diffusion is due to the Fermi level effect and self-interstitial supersaturation rather than transient effects resulting from implantation damage.

DISCUSSION

Figure 2 shows a plot of the self- and B diffusion coefficients as a function of reciprocal temperature. Extrinsic self- and dopant diffusion coefficients are reported for the maximum B concentration (i.e., at the amorphous/crystalline interface) at each temperature. Since the interface acts as a nearly ideal source and sink for native defects, the data in Figure 3 represent the pure Fermi level diffusion enhancement, independent of supersaturation effects.

To compare the B diffusivity data to literature values, the diffusion coefficients were reduced to intrinsic conditions by applying:

$$D_B(n_i) = D_B(p) \times n_i / C_B^{eq} \qquad (5)$$

where n_i represents the intrinsic carrier concentration at the diffusion temperature and C_B^{eq} is the B concentration at the amorphous/crystalline interface. The diffusion coefficients of B reduced to intrinsic conditions are consistent with corresponding data reported in the literature [16]. This reveals that B and Si diffusion are not enhanced by transient diffusion phenomena which may be associated with crystallization of the B implanted amorphous Si layer or implantation damage.

Comparison of simulation results to experimental data revealed that the interstitialcy mechanism is not possible for $[BI]^0$ correlation factors greater than 0.3. Although the experimental results may be explained using the reaction mechanism given by Eq. 2, such a low correlation factor renders the interstitialcy mechanism very unlikely. A theoretical calculation of the $[BI]^0$ correlation factor will be necessary to positively confirm this conclusion.

Figure 3(a) illustrates that the Si self-diffusion coefficient under heavy B doping, $D_{Si}(p)$, is clearly enhanced compared to the Si self-diffusion coefficient under intrinsic conditions, $D_{Si}(n_i)$. The neutral and singly positively charged interstitial contributions to the overall self-diffusion coefficient as a function of temperature are also shown in this figure. Singly positively charged

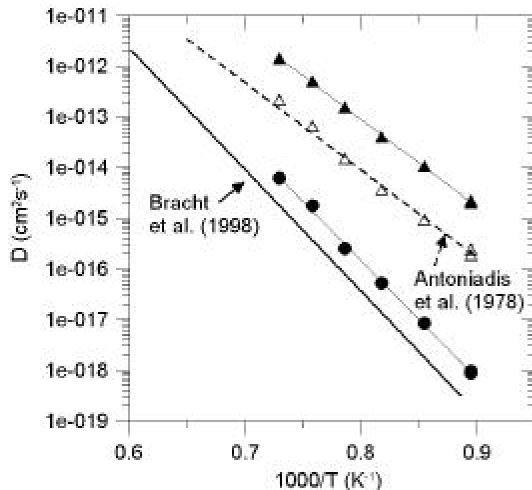

Figure 2: Extrinsic B(▲) and Si (●) diffusivities as a function of reciprocal temperature show a clear enhancement over literature values for intrinsic B [16] and Si [5] diffusion. B diffusivity data, reduced to intrinsic conditions (Ä), are in excellent agreement with intrinsic B diffusivities reported by Antoniadis et al. [16].

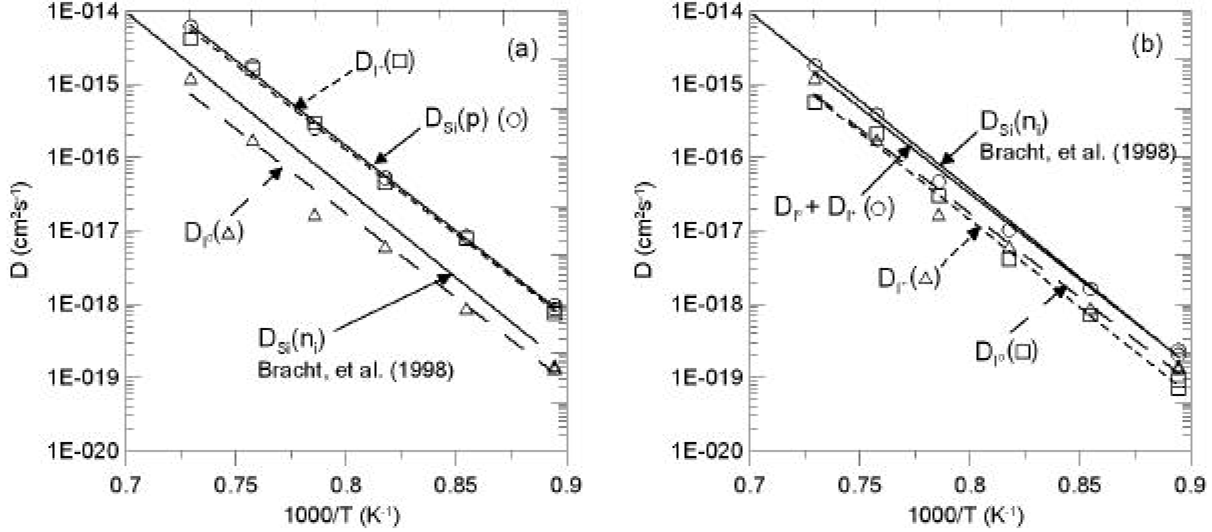

Figure 3: Individual contributions of neutral and singly positively charged self- interstitials to the Si self-diffusion coefficient and the sums of those contributions for (a) extrinsic and (b) intrinsic conditions. The data for figure (b) are obtained by reducing the extrinsic diffusivities obtained from the simulation to intrinsic conditions. This method allowed for the calculation of the individual Arrhenius parameters for I^0 and I^+ in intrinsic Si.

interstitials are responsible for the enhancement of Si self-diffusion. Figure 3(b) shows the defect diffusivities reduced to intrinsic conditions. The temperature dependences of the reduced diffusivities of neutral and singly positively charged interstitials are described by the following Arrhenius expressions:

$$D_{I^0}(n_i) = (44^{+379}_{-39}) \exp\left(-(4.56 \pm 0.241 \text{ eV})/kT\right) \text{ cm}^2 \text{ s}^{-1} \quad (6)$$

$$D_{I^+}(n_i) = (177^{+434}_{-126}) \exp\left(-(4.74 \pm 0.13 \text{ eV})/kT\right) \text{ cm}^2 \text{ s}^{-1}. \quad (7)$$

The sum of the contributions of D_I^0 and D_I^+ to Si self-diffusion is shown in Figure 3(b). The sum is in close agreement with data for Si diffusion under intrinsic conditions [5]. The overall consistency of the Si and B intrinsic diffusion data with corresponding data in the literature supports the diffusion reaction mechanisms considered for simultaneous diffusion of B and Si.

Our experiments aimed to better understand the mechanism for self- and dopant diffusion in extrinsic Si. TED effects from ion implantation would make it impossible to isolate the effect of charged interstitials. To reproduce the damage caused by B implantation, additional samples were implanted with Si and annealed. The resulting values for Si diffusivity as a function of reciprocal temperature data are in close agreement with previously determined Si self-diffusion data [5] (see [17]). Therefore, the observed diffusion enhancement in extrinsically B doped Si is due to the Fermi level effect rather than transient effects.

CONCLUSION

Self- and dopant diffusion experiments were performed using Si isotope multilayer structures. Simultaneous analysis of B and Si diffusion profiles allowed for determination of the diffusion mechanism and the individual contributions and charge states of the defects involved.

We conclude that B diffusion occurs via the kick-out mechanism and that the interstitialcy mechanism is highly unlikely. A theoretical calculation of the correlation factor of the $[BI]^0$ pair would be helpful.

Neutral and singly positively charged self- interstitials mediate self- and dopant diffusion. Observed diffusion enhancements under extrinsic conditions arise from increased singly positively charged interstitial concentrations due to the Fermi level effect and interstitial supersaturation due to B diffusion. Substantial vacancy contributions to diffusion were not observed. The Arrhenius expressions for the individual diffusion coefficients of neutral and singly positively charged interstitials in intrinsic Si were obtained from reduction of extrinsic data to intrinsic conditions. Additional results obtained from diffusion experiments with the n-type dopant As are given in these proceedings [17]. P and Sb diffusion experiments are currently in progress. Combining all results from these experiments will provide a comprehensive model of self- and dopant diffusion in Si.

ACKNOWLEGMENTS

This work was supported in part by industry and the State of California under the UC-SMART program No. SM97-01, by US NSF Grant No. DMR-0109844, and by the Director, Office of Science, Office of Basic Energy Sciences, Division of Materials Sciences and Engineering, of the U.S. Department of Energy under Contract No. DE-AC03-76SF00098.

REFERENCES

[1] R.F. Peart, Phys. Stat. Sol. **15** K119 (1966).
[2] B.J. Masters and J.M. Fairfield, Appl. Phys. Lett. **8** 280 (1960).
[3] J.M. Fairfield and B.J. Masters, J. Appl. Phys. **38** 3148 (1967).
[4] H.J. Mayer, H. Mehrer, and K. Maier, Inst. Phys. Conf. Ser. **31** 186 (1977).
[5] H. Bracht, E.E. Haller, and R. Clark-Phelps, Phys. Rev. Lett. **81** 393 (1998).
[6] A. Ural, P.B. Griffin, and J.D. Plummer, Phys. Rev. Lett. **83** 3454 (1999).
[7] Y. NakaBayashi, H.J. Osman, T. Segawa, K. Saito, S. Matsumoto, J. Murota, K. Wada, and T. Abe, Jpn. J. Appl. Phys. **39** 1133 (2000).
[8] A. Ural, P.B. Griffin, and J.D. Plummer, Appl. Phys. Lett. **79** 4328 (2001).
[9] W. Shockley and J.L. Moll, Phys. Rev. **119** 1480 (1960).
[10] D.J. Eaglesham, P.A. Stolk, H.-J. Gossman, and J.M. Poate, Appl. Phys. Lett. **65** 2305 (1994).
[11] P.M. Fahey, P.B. Griffin, and J.D. Plummer, Reviews of Modern Physics, **61** 289 (1989).
[12] W. Jüngling, P. Pichler, S. Selberherr, E. Guerro, and H. W. Pötzl, IEEE Trans. Electron. Devices ED **32** 156 (1985).
[13] N.E.B. Cowern, M.J.J. Theunuissen, F. Roozeboom, and J.G.M. van Berkum, App. Phys. Lett. **75** 181 (1999).
[14] B. Sadigh, T.J. Lenosky, S.K. Theiss, M.J. Caturla, T. Diaz de la Rubia, and M.A. Foad, Phys. Rev. Lett. **83** 4341 (1999).
[15] W. Windl, M.M. Bunea, R. Stumpf, S.T. Dunham, and M.P. Masquelier, Phys. Rev. Lett. **83** 4345 (1999).
[16] D.A. Antoniadis, A.G. Gonzalez, and R.W. Dutton, J. Electrochem. Soc. **125** 813 (1978).
[17] H.H. Silvestri et al., these proceedings.